Effects of Location Awareness on Concurrent Transmissions for Cognitive Ad Hoc Networks Overlaying Infrastructure-Based Systems

Li-Chun Wang, *Senior Member*, *IEEE*, and Anderson Chen, *Student Member*, *IEEE*

Abstract—Through wideband spectrum sensing, cognitive radio (CR) can identify the opportunity of reusing the frequency spectrum of other wireless systems. To save time and energy of wideband spectrum, we investigate to what extent a CR system incorporating the location awareness capability can establish a scanning-free region where a peer-to-peer ad hoc network can overlay on an infrastructure-based network. Based on the carrier sense multiple access with collision avoidance (CSMA/CA) medium access control (MAC) protocol, the concurrent transmission probability of a peer-to-peer connection and an infrastructure-based connection is computed. It is shown that the frequency band of the legacy system can be reused up to 45 percent by the overlaying cognitive ad hoc network when CR users have the location information of the primary and secondary users.

Index Terms—Ad hoc networks, cognitive radio, carrier sense multiple acces, MAC protocol.

1 Introduction

Cognitive radio (CR) has attracted a great deal of attention from both academia and industry recently because unlicensed spectrums become very crowded but some licensed spectrums are not fully utilized [1], [2]. In addition to Federal Communication Council [3], the Defense Advance Research Projects Agency (DARPA) also initiates the next-generation communications (XG) program to develop the so-called *opportunistic spectrum access* techniques for military and emergency applications [4]. The authors in [5] and [6] provide inspiring and comprehensive overviews on the related research issues in a CR system. To establish a harmless communication link in the presence of the existing legacy systems, a CR user is required to

1. sense wideband spectrums [7], [8], [9],
2. identify the primary user's spectrum usage in terms of locations and time [10], [11], [12], [13], [14], and
3. realize the spectrum sharing opportunities between the primary and secondary users by adjusting the transmission parameters accordingly [15], [16], [17], [18], [19], [20].

However, wideband spectrum sensing requires sophisticated and energy-consuming signal processing [16].

Instead of developing another efficient spectrum sensing technique, in this paper, we discuss a challenging but fundamental issue—Can CR users effectively identify the available spectrum holes without wideband spectrum sensing? Intuitively, when the secondary CR users are far away from the primary user of the legacy system, both CR and the primary users can concurrently transmit their data without causing interference. If a CR device knows the region where it can concurrently transmit with the primary user, a CR system does not need to rely on the time- and energy-consuming wideband spectrum scanning to detect the spectrum holes. In addition, it is clear that concurrent transmission can enhance the overall throughput. In this sense, identifying concurrent transmission opportunity shall be given a higher priority over spectrum sensing for a CR user.

The next important issue is how to identify the concurrent transmission region where CR users will not cause interference to the legacy wireless systems. In this paper, we propose to utilize the location awareness techniques to help CR users identify the concurrent transmission opportunity. Our specific goal is to dimension the concurrent transmission region where CR devices can establish an overlaying ad hoc network on top of an infrastructure-based legacy system. The overlaying ad hoc network can be considered an important application for CR devices because it can reuse the underutilized spectrum and significantly improve the efficiency of the frequency band. A possible example is that a group of users who want to share data with each other may require to set up such an overlaying ad hoc network. Suppose that their communication devices only can access the licensed spectrum. Obviously, all of them may not want to pay just for a temporary data transfer. To solve this situation, an overlaying ad hoc link in the presence of primary connection may be the network architecture that can satisfy their requirement. We believe this network topology will become more and more attractive because of the spectrum scarcity as the advance of the wireless technology. We will also investigate the throughput improvement resulting from concurrent transmissions based on the carrier sense multiple access with collision avoidance (CSMA/CA) medium access control (MAC) protocol.

In the literature, the coexistence issue of the hybrid infrastructure-based and overlaying ad hoc networks has

• *The authors are with the Department of Communication Engineering, National Chiao-Tung University, 1001 Ta Hsueh Road, Hsinchu 300, Taiwan, ROC.*
E-mail: lichun@cc.nctu.edu.tw, mingbing.cm87g@nctu.edu.tw.

Manuscript received 19 Jan. 2007; revised 13 Dec. 2007; accepted 20 Feb. 2008; published online 25 Apr. 2008.
For information on obtaining reprints of this article, please send e-mail to: tmc@computer.org, and reference IEEECS Log Number TMC-0023-0107.
Digital Object Identifier no. 10.1109/TMC.2008.72.

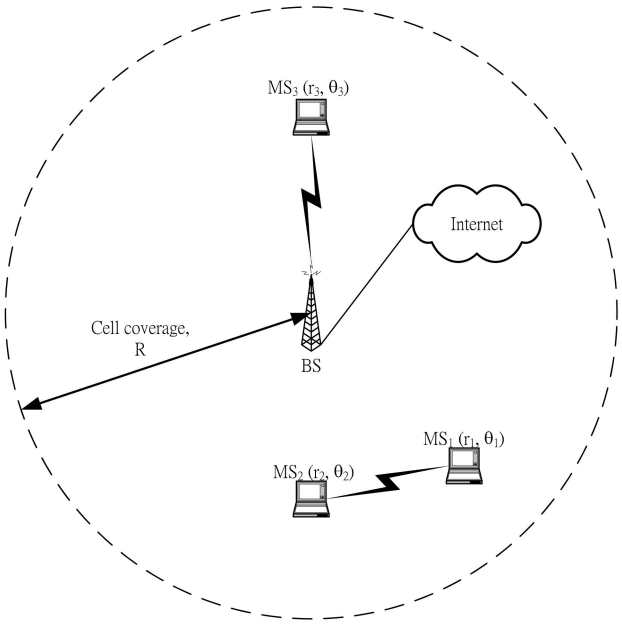

Fig. 1. An illustrative example for the coexistence of two CR devices establishing a peer-to-peer ad hoc link and a primary user connecting to the infrastructure-based network, where all the devices (MS_1, MS_2, and MS_3) use the same spectrum simultaneously.

been addressed but in different scenarios. In [21], [22], [23], and [24], the idea of combining ad hoc link and infrastructure-based link was proposed mainly to extend the coverage area of the infrastructure-based network. That is, the coverage area of ad hoc networks is not overlapped with that of the infrastructure-based network. In the present hybrid ad hoc/infrastructure-based network, as shown in Fig. 1, the peer-to-peer CR users are located within the coverage area of the existing legacy wireless network. In [25], to further improve the throughput of a wireless local area network (WLAN), it was suggested that an access point (AP) could dynamically switch between the infrastructure mode and the ad hoc mode. In our considered scenario, the decision of establishing ad hoc connections is made by the CR users in a distributed manner.

The main contribution of this paper is to provide the idea of utilizing location awareness to facilitate frequency sharing in a concurrent transmission manner. Specific achievements are summarized in the following:

- We show that a CR device having location information of other nodes can concurrently transmit a peer-to-peer data in the presence of an infrastructure-based connection in some region. We also dimension the concurrent transmission (or the scanning-free) region for CR users. Note that a concurrent transmission region of a CR system is equivalent to a scanning-free region. Nevertheless, the wideband spectrum sensing procedure is still needed but is initiated only when the CR user is outside the concurrent transmission region. Therefore, the energy consumption of CR systems with location awareness capability can be reduced significantly.
- Based on the CSMA/CA MAC protocol, a physical/MAC cross-layer analytical model is developed to compute the coexistence probability of a peer-to-peer connection and an infrastructure-based connection. Based on this analytical model, we find that concurrent transmission of the secondary CR users and the primary users in the legacy system can significantly enhance the total throughput over the pure legacy system.

The rest of this paper is organized as follows: Section 2 describes the system model. Section 3 analyzes the coexistence probability of both the infrastructure and ad hoc modes sharing the same frequency spectrum simultaneously. The impacts of shadowing on this coexistence probability are investigated in Section 4. The physical (PHY) and MAC cross-layer performance analysis is provided in Section 5. Section 6 shows the numerical results. The concluding remarks are given in Section 7.

2 System Model and Definition

Fig. 1 illustrates a hybrid ad hoc/infrastructure-based network consisting of two CR devices (MS_1 and MS_2) and a primary user MS_3. Assume that the secondary CR users MS_1 and MS_2 try to make a peer-to-peer connection, and the primary user MS_3 has been connected to the base station (BS) or AP of the legacy infrastructure-based system. In the figure, MS_1, MS_2, and MS_3 are located at (r_1, θ_1), (r_2, θ_2), and (r_3, θ_3), respectively; the coverage area of the BS is πR^2. All the primary and secondary users stay fixed or hardly move.

We assume that the CR devices can perform the positioning technique to acquire their relative or absolute position by using GPS or detecting the signal strength from the BSs of legacy systems [26], [27], [28], [29], [30], [31]. The location information is broadcasted by using the geographical routing protocols [32], [33], [34]. Although both the positioning and geographical routing may waste time and consume energy, they have no need to be processed for every data transmission. They are only performed when a new node joins or the node changes its position. Furthermore, with the help of upper layers, the location information is already stored in the device. Therefore, compared to the spectrum sensing at every transmission, we believe that the additional energy consumption and memory space due to the positioning and location update is relatively small. The overhead and optimal reserved resources for acquiring the location information are beyond the scope of this paper, but the relative research works have been studied in [35] and [36].

Based on the CSMA/CA MAC protocol, multiple users contend the channel, and only one mobile station within the coverage of the BS can establish an infrastructure-based communication link at any instant. To set up an extra peer-to-peer ad hoc connection in the same frequency band of the primary user, the secondary users not only require to ensure that the current infrastructure-based link quality cannot be degraded but also has to win the contentions between other feasible secondary users. Here, we consider that both primary and secondary users have identical transmit power. It is reasonable to assume that only one secondary user can establish a link after the contention at one instance due to the similar interference range. Denote SIR_i and SIR_a as the received signal-to-interference ratios (SIRs) of the infrastructure-based and ad hoc links, respectively. Then, we can define the coexistence (or concurrent

transmission) probability (P_{CT}) of the infrastructure-based link and CR-based ad hoc link in an overlapped area as follows:

$$P_{CT} = P\{(SIR_i > z_i) \cap (SIR_a > z_a)\}, \quad (1)$$

where z_i and z_a are the required SIR thresholds for the infrastructure-based and ad hoc links, respectively. To obtain the concurrent transmission region, it is crucial to calculate the coexistence probability of both the infrastructure and ad hoc links. If the link quality of the primary user cannot be guaranteed, CR devices have to sense and change to other frequency bands.

We consider the two-ray ground reflection model in which there exists two paths between the transmitter and receiver [37]. One is the line-of-sight, and the other is reflected from ground. Thus, the received power can be written as

$$P_r = \frac{P_t h_{bs}^2 h_{ms}^2 G_{bs} G_{ms} 10^{\frac{\xi}{10}}}{r^{\alpha}}, \quad (2)$$

where P_r and P_t are the received and transmitted power levels at a mobile station, respectively; h_{bs} and h_{ms} represent the antenna heights of the BS and the mobile station, respectively; G_{bs} and G_{ms} stand for the antenna gains of the BS and the mobile station, respectively; r is the distance between the transmitter and receiver; α is the path loss exponent; and $10^{\xi/10}$ is the lognormally distributed shadowing component.

3 Signal-to-Interference Ratio Analysis

3.1 Uplink SIR Analysis

In the *uplink case*, when the primary user MS_3 transmits data to the BS, denote $SIR_i^{(u)}$ as the uplink SIR of MS_3 and let P_{30} and P_{10} be the received power from MS_3 and MS_1 at the BS, respectively. Then, from (2), we have

$$SIR_i^{(u)} = \left(\frac{r_1}{r_3}\right)^{\alpha} = \frac{P_{30}}{P_{10}}, \quad (3)$$

where r_1 and r_3 are the distances between MS_1 and MS_3 to the BS, respectively. Similarly, the SIR of a peer-to-peer ad hoc link from MS_1 to MS_2 can be written as

$$SIR_a = \frac{P_{12}}{P_{32}} = \left(\frac{d_{23}}{d_{12}}\right)^{\alpha}, \quad (4)$$

where P_{12} is the received power at MS_2 from MS_1 and P_{32} is the interference power from MS_3; d_{12} and d_{23} are the distances from MS_1 and MS_3 to MS_2, respectively. Substituting (3) and (4) into (1), the concurrent transmission probability $P_{CT}^{(u)}$ in the *uplink case* can be written as

$$P_{CT}^{(u)} = P\left\{\left(r_3 z_i^{1/\alpha} < r_1 < R\right) \cap \left(d_{12} < \frac{d_{23}}{z_a{}^{1/\alpha}}\right)\right\} \triangleq \frac{R_{CT}^{(u)}}{\pi R^2}. \quad (5)$$

Note that $R_{CT}^{(u)}$ denotes the concurrent transmission region where MS_1 can connect to MS_2 without interfering the uplink signal of MS_3 to the BS. As shown in Fig. 2, the condition $(r_3 z_i^{1/\alpha} < r_1 < R)$ leads to a donut-shaped area consisting of two circles centered at the BS with the radii of $r_3 z_i^{1/\alpha}$ and R, respectively. Meanwhile, the condition $(d_{12} < d_{23}/z_a^{1/\alpha})$ yields the circular area centering at MS_2 with a radius of $d_{23}/z_a^{1/\alpha}$. From the figure, the region $R_{CT}^{(u)}$ can be computed as

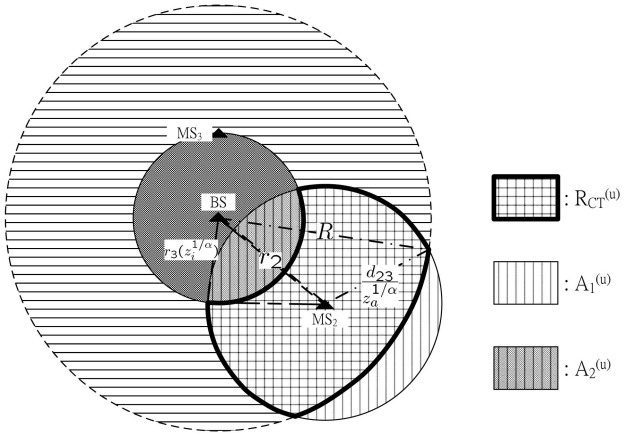

Fig. 2. Physical representation of the coexistence probability for the concurrent transmission of hybrid CR-based ad hoc link and infrastructure uplink transmission.

$$R_{CT}^{(u)} = \pi\left(\frac{d_{23}}{z_a^{1/\alpha}}\right)^2 - A_1 - A_2, \quad (6)$$

where

$$A_1 = \left(\frac{d_{23}}{z_a^{1/\alpha}}\right)^2 (\pi - \theta') - R^2\theta + 2\Delta \quad (7)$$

and

$$A_2 = \left(\frac{d_{23}}{z_a^{1/\alpha}}\right)^2 \phi - \left(r_3 z_i^{1/\alpha}\right)^2 \phi' - 2\Delta'. \quad (8)$$

The definitions of parameters θ, θ', ϕ, ϕ', Δ, and Δ' and the detailed derivation of (6), (7), and (8) are discussed in Appendix A.

3.2 Downlink SIR Analysis

Now, we consider the *downlink case* when the BS sends data to the primary user MS_3. Denote $SIR_i^{(d)}$ as the infrastructure link's SIR in the downlink direction. Then, from (2), we have

$$SIR_i^{(d)} = \frac{P_{03}}{P_{13}} = \left(\frac{h_{bs}}{h_{ms}}\right)^2 \left(\frac{d_{13}}{r_3}\right)^{\alpha}, \quad (9)$$

where P_{03} and P_{13} are the MS_3's received powers from the BS and MS_1, respectively; d_{13} stands for the distance from MS_1 to MS_3; h_{bs}, h_{ms}, and r_3 are given in (2) and (3). Similarly, the ad hoc link's SIR from MS_1 to MS_2 can be expressed as

$$SIR_a = \frac{P_{12}}{P_{02}} = \left(\frac{h_{ms}}{h_{bs}}\right)^2 \left(\frac{r_2}{d_{12}}\right)^{\alpha}, \quad (10)$$

where P_{12} and P_{02} are the received powers at MS_2 from MS_1 and the BS, respectively; r_2 represents the distance between MS_2 and the BS; d_{12}, h_{bs}, and h_{ms} are defined in (4) and (2).

Substituting (9) and (10) into (1), we can obtain the concurrent transmission probability $P_{CT}^{(d)}$ of a CR-based

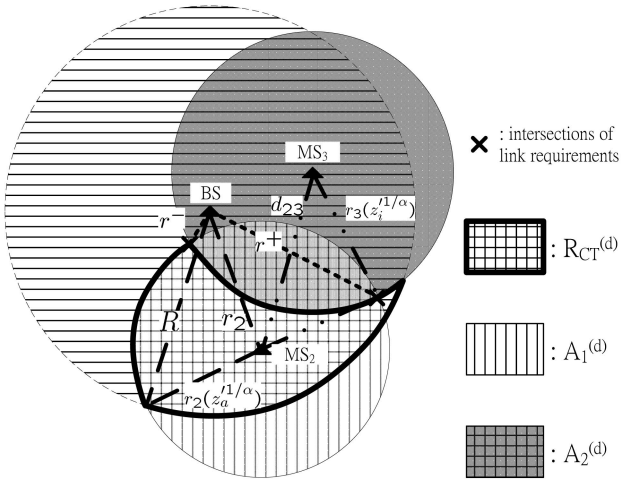

(a)

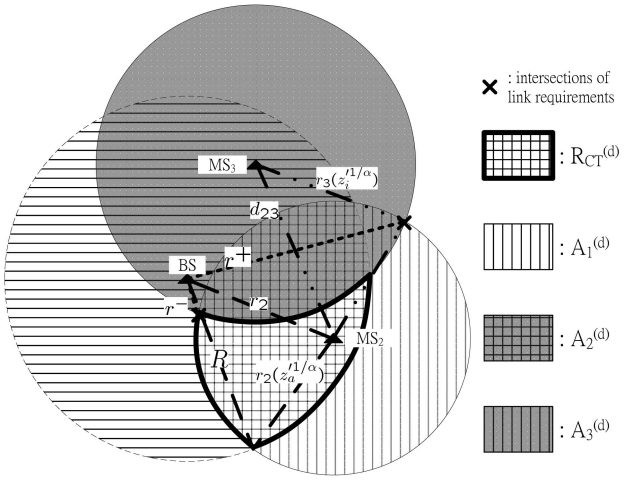

(b)

Fig. 3. The area of concurrent transmission region R_{CT} in downlink cases. (a) The case when $\max(r^+, r^-) \leq R$. (b) The case when $\max(r^+, r^-) > R$.

peer-to-peer ad hoc link and an infrastructure-based downlink transmission as follows:

$$P_{CT}^{(d)} = P\left\{\left(d_{13} > r_3 z_i'^{1/\alpha}\right) \cap \left(d_{12} < r_2 z_a'^{1/\alpha}\right) \cap (r_1 < R)\right\} \triangleq \frac{R_{CT}^{(d)}}{\pi R^2}, \tag{11}$$

where $z_i' = z_i \cdot (h_{ms}^2/h_{bs}^2)$, and $z_a' = (1/z_a) \cdot (h_{ms}^2/h_{bs}^2)$. From (11), the concurrent transmission region $R_{CT}^{(d)}$ in the *downlink case* is shown in Fig. 3. The criterion $(d_{13} > r_3 z_i'^{1/\alpha})$ results in the region outside the circle centered at MS_3 with a radius of $r_3 z_i'^{1/\alpha}$, while the criterion $(d_{12} < r_2 z_a'^{1/\alpha})$ yields the region inside the circle centered at MS_2 with radius $r_2 z_a'^{1/\alpha}$. At last, $r_1 < R$ because MS_1 is assumed to be uniformly distributed within a cell of radius R.

The coexistence probability of the CR-based ad hoc link and the infrastructure-based downlink can be obtained by calculating the area of $R_{CT}^{(d)}$. The distances from the AP to the intersections of the two circles with radii of $r_3 z_i'^{1/\alpha}$ and $r_2 z_a'^{1/\alpha}$ are denoted by r^+ and r^- as shown in Fig. 3. In Appendix B, we have shown that

$$r^+ = \frac{1}{d_{23}^2}\left\{\sin(\theta_2 - \theta_3)\delta + r_2 r_3\left[r_2 r_3\left(z_a'^{\frac{2}{\alpha}} + z_i'^{\frac{2}{\alpha}}\right) + \cos(\theta_2 - \theta_3)\left(d_{23}^2 - r_2^2 z_a'^{\frac{2}{\alpha}} - r_3^2 z_i'^{\frac{2}{\alpha}}\right)\right]\right\} \tag{12}$$

and

$$r^- = -\frac{1}{d_{23}^2}\left\{\sin(\theta_2 - \theta_3)\delta - r_2 r_3\left[r_2 r_3\left(z_a'^{\frac{2}{\alpha}} + z_i'^{\frac{2}{\alpha}}\right) + \cos(\theta_2 - \theta_3)\left(d_{23}^2 - r_2^2 z_a'^{\frac{2}{\alpha}} - r_3^2 z_i'^{\frac{2}{\alpha}}\right)\right]\right\}, \tag{13}$$

where

$$\delta = \sqrt{2r_3^2 z_i'^{\frac{2}{\alpha}}\left(d_{23}^2 + r_2^2 z_a'^{\frac{2}{\alpha}}\right) - \left(d_{23}^2 - r_2^2 z_a'^{\frac{2}{\alpha}}\right)^2 - r_3^4 z_i'^{\frac{4}{\alpha}}}. \tag{14}$$

With the values of r^+ and r^-, $R_{CT}^{(d)}$ can be calculated in the following two cases:

1. $\max(r^+, r^-) \leq R$: In this case, referring to Fig. 3a, the area of $R_{CT}^{(d)}$ can be expressed as

$$R_{CT}^{(d)} = \pi\left(d_{23} z_a'^{1/\alpha}\right)^2 - A_1 - A_2, \tag{15}$$

where

$$A_1 = \left(r_2 z_a'^{1/\alpha}\right)^2(\pi - \theta') - R^2\theta + 2\Delta, \tag{16}$$

$$A_2 = \left(r_2 z_a'^{1/\alpha}\right)^2\phi - \left(r_3 z_i'^{1/\alpha}\right)^2\phi' - 2\Delta'. \tag{17}$$

2. $\max(r^+, r^-) > R$: As shown in Fig. 3b, the area of $R_{CT}^{(d)}$ can be expressed as

$$R_{CT}^{(d)} = \pi\left(d_{23} z_a'^{1/\alpha}\right)^2 - A_1 - A_2 + A_3, \tag{18}$$

where

$$A_1 = \left(r_2 z_a'^{1/\alpha}\right)^2(\pi - \theta') - R^2\theta + 2\Delta, \tag{19}$$

$$A_2 = \left(r_2 z_a'^{1/\alpha}\right)^2\phi - \left(r_3 z_i'^{1/\alpha}\right)^2\phi' - 2\Delta', \tag{20}$$

$$A_3 = \Delta'' + \left[\left(r_3 z_i'^{1/\alpha}\right)^2\psi_2 - \frac{1}{2}\left(r_3 z_i'^{1/\alpha}\right)^2\sin\psi_2\right] + \left[\left(r_2 z_a'^{1/\alpha}\right)^2\psi_3 - \frac{1}{2}\left(r_2 z_a'^{1/\alpha}\right)^2\sin\psi_3\right] - \left[R^2\psi_1 - \frac{1}{2}R^2\sin\psi_1\right]. \tag{21}$$

The detailed derivations of (15) and (18) and the definitions of the parameters θ, θ', ϕ, ϕ', ψ_1, ψ_2, ψ_3, Δ, Δ', and Δ'' are given in Appendices C and D, respectively.

3.3 Multiple Ad Hoc Connections Coexisting with One Infrastructure Link

After evaluating the concurrent transmission probability of the infrastructure link and the one overlaying CR-based ad hoc link, one may be interested in knowing how many secondary users can concurrently establish ad hoc links together with the primary user. This question is nontrivial since it needs to consider the interference from a set of ad hoc links to the infrastructure link, and vice versa. Besides, different from the pure infrastructure network, both the locations of the transmitter and receiver in an ad hoc link are random.

Instead of calculating the maximum number of ad hoc links, we suggest constructive procedures enabling CR devices to establish ad hoc links in the presence of an infrastructure transmission. The detailed procedures are summarized as follows:

1. Consider a network in which all the primary and secondary users are fixed, and the CR device can learn the locations of its receiver and neighbors by the routing mechanism [17]. Here, we assume that l ad hoc links have been established and coexisted with the infrastructure link at the same time. Before establishing a new ad hoc connection, the CR device has to overhear the channel and memorize the locations of all the existing transmitters.
2. With the location information, the new CR device starts evaluating the concurrent transmission region R_{CT}. The device should consider the interference from the infrastructure link as well as other existing ad hoc links, and vice versa. Denote the indices $\{p, m, n, k\}$ as the primary user, the transmitter and receiver of the new ad hoc link, and the transmitter of other existing ad hoc link, respectively. Using similar procedures in deriving (5), the three conditions in the infrastructure uplink case can be written by

$$r_m \geq \left(\frac{1}{\frac{1}{z_i}\left(\frac{1}{r_p}\right)^{\alpha} - \sum_k \left(\frac{1}{r_k}\right)^{\alpha}} \right)^{\frac{1}{\alpha}}, \tag{22}$$

$$d_{mn} \leq \left(\frac{1}{z_a\left(\left(\frac{1}{d_{pm}}\right)^{\alpha} + \sum_k \left(\frac{1}{d_{kn}}\right)^{\alpha}\right)} \right)^{\frac{1}{\alpha}}, \tag{23}$$

$$r_m \leq R, \tag{24}$$

where r_i and d_{ij} are the distances between the BS and CR device j to i, respectively. Similarly, from (11), the three criteria in the downlink case are

$$d_{mp} \geq \left(\frac{1}{\frac{1}{z_i}\left(\frac{1}{r_p}\right)^{\alpha} - \sum_k \left(\frac{1}{d_{kp}}\right)^{\alpha}} \right)^{\frac{1}{\alpha}}, \tag{25}$$

$$d_{mj} \leq \left(\frac{1}{z_a\left(\left(\frac{1}{r_n}\right)^{\alpha} + \sum_k \left(\frac{1}{d_{kn}}\right)^{\alpha}\right)} \right)^{\frac{1}{\alpha}}, \tag{26}$$

$$r_m \leq R. \tag{27}$$

3. Since the concurrent transmission regions $R_{CT}^{(u)}$ and $R_{CT}^{(d)}$ are known, the CR device can determine whether it can concurrently transmit data together with the infrastructure link and other ad hoc connections by the primary user and other secondary CR users.

4 Shadowing Effects

In the previous section, we only consider the impact of path loss on the concurrent transmission probability of CR-based network overlaying the infrastructure-based system. However, even though the CR device is located inside the concurrent transmission region R_{CT}, a peer-to-peer ad hoc connection may not be able to coexist together with the primary user's infrastructure link due to shadowing. Thus, it is important to investigate the reliability of concurrent transmissions of the hybrid infrastructure and CR-based ad hoc network when shadowing is taken into account.

Shadowing can be modeled by a lognormally distributed random variable [38]. Represent $10^{\xi_{ij}/10}$ as the shadowing component in the propagation path from users i to j, where ξ_{ij} is a Gaussian random variable with zero mean and standard deviation of σ_ξ. Thus, the uplink and downlink SIRs in both the infrastructure-based connection and CR-based ad hoc link are modified as follows:

- *uplink case:*

$$SIR_i^{(u)}(\xi_{30}, \xi_{10}) = \frac{10^{\frac{\xi_{30}}{10}}/r_3^{\alpha}}{10^{\frac{\xi_{10}}{10}}/r_1^{\alpha}}, \tag{28}$$

$$SIR_a^{(u)}(\xi_{12}, \xi_{32}) = \frac{10^{\frac{\xi_{12}}{10}}/d_{12}^{\alpha}}{10^{\frac{\xi_{32}}{10}}/d_{23}^{\alpha}}, \tag{29}$$

- *downlink case:*

$$SIR_i^{(d)}(\xi_{03}, \xi_{13}) = \frac{10^{\frac{\xi_{03}}{10}}/r_3^{\alpha}}{10^{\frac{\xi_{13}}{10}}/d_{13}^{\alpha}}, \tag{30}$$

$$SIR_a^{(d)}(\xi_{12}, \xi_{02}) = \frac{10^{\frac{\xi_{12}}{10}}/d_{12}^{\alpha}}{10^{\frac{\xi_{02}}{10}}/r_2^{\alpha}}. \tag{31}$$

Note that the index 0 represents the BS and ξ_{30} of (29) in the uplink case is equivalent to ξ_{03} of (31) in the downlink case. Let $\boldsymbol{\xi} = (\xi_{10}, \xi_{30}, \xi_{12}, \xi_{32})$ and $\boldsymbol{\xi}' = (\xi_{13}, \xi_{03}, \xi_{12}, \xi_{02})$ and assume that these shadowing components are identical and independently distributed. Taking shadowing into account, the concurrent transmission probability P_{CT} can be represented by

- *uplink case:*

$$P_{CT}^{(u)}(\boldsymbol{\xi}) = P\left\{ \left(r_3\left(z_i 10^{\frac{\xi_{10}-\xi_{30}}{10}}\right)^{1/\alpha} < r_1 < R \right) \cap \left(d_{12} < d_{23}\left(z_a 10^{\frac{\xi_{12}-\xi_{32}}{10}}\right)^{1/\alpha} \right) \right\}, \tag{32}$$

- *downlink case:*

$$P_{CT}^{(d)}(\boldsymbol{\xi}') = P\Bigg\{ \left(d_{13} > r_3 \left(z_i 10^{\frac{\xi_{13}-\xi_{03}}{10}} \right)^{1/\alpha} \right) \cap \left(d_{12} < r_2 \left(z_a 10^{\frac{\xi_{12}-\xi_{02}}{10}} \right)^{1/\alpha} \right) \cap (r_1 < R) \Bigg\}. \tag{33}$$

We define the reliability of uplink concurrent transmission $F_{CT}^{(u)}(\xi)$ as the probability that, in the region R_{CT}, a CR device can successfully establish an ad hoc link in the presence of the primary user's uplink transmission subject to the shadowing effect. That is,

$$F_{CT}^{(u)}(\boldsymbol{\xi}) = P\Bigg\{ \left(SIR_i^{(u)}(\xi_{30}, \xi_{10}) > z_i \right) \cap \left(SIR_a^{(u)}(\xi_{12}, \xi_{32}) > z \right) | \mathrm{MS}_1 \in R_{CT}^{(u)} \Bigg\}. \tag{34}$$

Note that $F_{CT}^{(u)}(\boldsymbol{\xi}) = 1$ when shadowing is not considered. Substituting (28) and (29) into (34), we can obtain

$$F_{CT}^{(u)}(\boldsymbol{\xi}) = P\Bigg\{ \left(\xi_{30} - \xi_{10} > 10 \log_{10} \left(z_i \left(\frac{r_3}{r_1} \right)^{\alpha} \right) \right) \cap \left(\xi_{12} - \xi_{32} > 10 \log_{10} \left(z_a \left(\frac{d_{12}}{d_{23}} \right)^{\alpha} \right) \right) | \mathrm{MS}_1 \in R_{CT}^{(u)} \Bigg\}. \tag{35}$$

Assume that ξ_{ij} have the same standard deviation for all i and j and let $\xi_i^{(u)} = \xi_{30} - \xi_{10}$, $\xi_a^{(u)} = \xi_{12} - \xi_{32}$. Then, $\xi_i^{(u)}$ and $\xi_a^{(u)}$ become Gaussian random variables with $\mathrm{N}(0, 2\sigma_\xi)$. Hence, it follows that

$$\begin{aligned} F_{CT}^{(u)}(\boldsymbol{\xi}) &= P\left\{ \xi_i^{(u)} \geq 10 \log_{10} \left(z_i \left(\frac{r_3}{r_1} \right)^{\alpha} \right) | \mathrm{MS}_1 \in R_{CT}^{(u)} \right\} \\ &\quad \cdot P\left\{ \xi_a^{(u)} \geq 10 \log_{10} \left(z_a \left(\frac{d_{12}}{d_{23}} \right)^{\alpha} \right) | \mathrm{MS}_1 \in R_{CT}^{(u)} \right\} \\ &= Q\left(\frac{10 \log_{10} \left(z_i \left(\frac{r_3}{r_1} \right)^{\alpha} \right)}{2\sqrt{2}\sigma} \right) \cdot Q\left(\frac{10 \log_{10} \left(z_a \left(\frac{d_{12}}{d_{23}} \right)^{\alpha} \right)}{2\sqrt{2}\sigma} \right), \end{aligned} \tag{36}$$

where $Q(x) = (1/\pi) \cdot \int_x^\infty \exp^{-x^2} dx$.

Following similar procedures in the uplink case, we can also obtain the reliability of downlink concurrent transmission as follows:

$$\begin{aligned} F_{CT}^{(d)}(\boldsymbol{\xi}') &= P\Bigg\{ \left(SIR_i^{(d)}(\xi_{03}, \xi_{13}) > z_i \right) \cap \left(SIR_a^{(d)}(\xi_{12}, \xi_{02}) > z \right) | \mathrm{MS}_1 \in R_{CT}^{(d)} \Bigg\} \\ &= Q\left(\frac{10 \log_{10} \left(z_i \left(\frac{r_3}{d_{13}} \right)^{\alpha} \right)}{2\sqrt{2}\sigma} \right) \cdot Q\left(\frac{10 \log_{10} \left(z_a \left(\frac{d_{12}}{r_2} \right)^{\alpha} \right)}{2\sqrt{2}\sigma} \right). \end{aligned} \tag{37}$$

5 MAC Layer Throughput Analysis

In this section, the MAC layer throughput performance of the considered hybrid infrastructure and overlaying CR-based ad hoc network is evaluated from a PHY/MAC cross-layer perspective. The main task here is to incorporate the interference from both the infrastructure and ad hoc links into the throughput evaluation model in the MAC layer.

In this paper, the CSMA/CA MAC protocol with the binary exponential back-off algorithm is considered because it is widely deployed in many license-exempt frequency bands. However, the CSMA/CA MAC protocol may not be used to establish the CR-based ad hoc link since the clear channel assessment (CCA) by measuring the received signal strength (RSS) may forbid the transmissions in the presence of infrastructure link. To remove this constraint, we use the location and channel station information to replace the RSS measurement for CCA in the traditional CSMA/CA MAC protocol. Therefore, the CR device can establish the ad hoc connection once the new connection does not injure the existing primary infrastructure link.

Next, we first summarize the calculation of saturation throughput in the traditional CSMA/CA MAC protocol [39], [40]. Assume N stations always transmit data packets in the network, and let W and $2^b W$ be the minimum and maximum back-off window sizes, respectively. Given the stationary transmission probability τ that a station transmits packet in a given slot and the successful transmission probability $p_s(N)$, the throughput $S(N)$ of the CSMA/CA MAC protocol can be expressed as [39], [40]

$$S(N) = \frac{p_{tr} p_s(N) \mathrm{E}[P]}{(1 - p_{tr})\sigma + p_{tr}(1 - p_s(N))T_c + p_{tr} p_s(N) T_c}, \tag{38}$$

where $p_{tr} = 1 - (1 - \tau)^N$; $\mathrm{E}[\mathrm{P}]$, T_s, T_c, and σ are the average payload size, the average successful transmission duration, the average collision duration, and the slot duration. Note that the average successful transmission and collision duration have included the DIFS and SIFS waiting time [39], [40]. The stationary transmission probability τ is a function of the packet loss probability p_L, that is

$$\tau(p_L) = \frac{2}{1 + W + p_L W \sum_{i=0}^{b-1} (2p_L)^i}. \tag{39}$$

Note that both the packet loss probability p_L and the successful transmission probability $p_s(N)$ are influenced by the radio channel effect and the multiuser capture effect in the physical layer [40].

Then, we evaluate the total throughput performance of the concurrent transmission in the hybrid infrastructure and overlaying CR-based ad hoc network. Here, we assume N_{CR} CR devices and N non-CR devices using the same frequency band in the coverage of a BS. Since the CR device can establish an ad hoc connection without interfering the existing infrastructure link, the total throughput of such a hybrid network S_{CT} is independently contributed by the two links. The throughput of the infrastructure link and the CR-based ad hoc connection are denoted by S_i and S_a, respectively. The total throughput S_{CT} can then be expressed as

$$S_{CT} = S_i(N) + S_a(N_{CR} P_{CT}). \tag{40}$$

TABLE 1
System Parameters

MAC/PHY header	224/192 bits
ACK/RTS/CTS	304/352/304 bits
DATA payload	16000 bits
Bit rate	1 Mbps
Slot time	$20\mu s$
SIFS/DIFS	$10/50\mu s$
Min contention window	32
Maximum backoff stage	5
Transmission power, P_t	20 dBm
Noise power, N_0	-90 dBm

Since N non-CR devices contend for data transmission to the BS, the throughput of infrastructure-based link S_i is the same as (38). As for the throughput of the cognitive overlaying ad hoc connection S_a, it is similar to S_i, but the number of contending stations changes to $N_{CR}P_{CT}$ because only $N_{CR}P_{CT}$ CR devices have the opportunity to establish the connection. Although the secondary user employs the location information to replace the carrier sensing in the CSMA/CA, it still needs to wait for the DIFS and SIFS durations and makes sure if other secondary users are transmitting data. Once the user finds another one establishes a link, it still has to freeze its back-off counter and resumes the back-off countdown after the link is complete, just like what the CSMA/CA MAC does. Therefore, all the throughput calculations for the secondary users is similar to that for the CSMA/CA MAC protocol. The only discrepancy between the two systems is merely the number of contending stations. Because only the secondary users within the same concurrent transmission region have the right to access the spectrum, the number of users for the overlaying ad hoc network is the function of the coexistence probability.

6 Numerical Results

In this section, we first investigate the concurrent transmission probability of the infrastructure and overlaying CR-based ad hoc network. Then, we apply the proposed cross-layer analytical model to evaluate the total throughput performance in this hybrid network. Fig. 1 illustrates the considered network topology, where MS_1, MS_2, and MS_3 are the CR-based ad hoc transmitter, receiver, and infrastructure primary user, respectively. The stations MS_2 and MS_3 are, respectively, located at $(r_2, -\pi/2)$ and $(r_3, \pi/2)$, where r_2 and r_3 are the distances between the BS to MS_2 and MS_3; whereas MS_1 is uniformly distributed in the cell with radius $R = 100$ m. In addition, we also perform the simulation to verify the proposed analytical model for the concurrent transmission probability P_{CT}. In the simulation, 10^4 points, which are uniformly distributed in the region πR^2, represent the possible locations of the ad hoc transmitter MS_1. The probability P_{CT} is calculated by counting the number of points where MS_1 can successfully establish an ad hoc link to MS_2 in the presence of the infrastructure link (BS to MS_3). As shown in the following figures, the results in the analytical model agrees well with that in the simulation. The other system parameters are listed in Table 1.

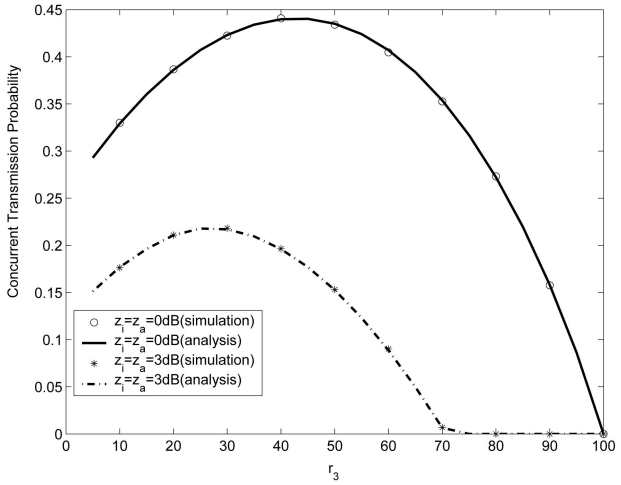

Fig. 4. The concurrent transmission probability $P_{CT}^{(u)}$ versus the infrastructure uplink user's locations as the ad hoc receiver MS_2 is located at $(50, -\pi/2)$, where r_3 is the distance between the BS and the primary user MS_3.

6.1 Uplink Concurrent Transmission Probability

Fig. 4 shows the impact of the primary user's location on the uplink concurrent transmission probability $P_{CT}^{(u)}$, where the transmission power $P_t = 20$ dBm and noise power $N_0 = -90$ dBm, respectively; the required link SIR threshold is 0 or 3 dB. First, one can see that the analytical results match the simulation results well. Second and more importantly, there exists an optimal concurrent transmission probability $P_{CT}^{(u)}$ against the distance r_3 from the primary user MS_3 to the BS. Note that, for $z_i = 0$ dB, the maximal $P_{CT}^{(u)} = 0.45$ at $r_3 = 40$ m, and for $z_i = 3$ dB, the maximal $P_{CT}^{(u)} = 0.22$ at $r_3 = 26$ m. This phenomenon can be explained as follows: On the one hand, when MS_3 approaches the BS, it is also closer to the CR-based ad hoc receiver, thereby causing higher interference and decreasing the concurrent transmission probability. On the other hand, when MS_3 moves away from the BS, its uplink SIR decreases due to the weaker signal strength and thus yields a lower $P_{CT}^{(u)}$. Hence, an optimal primary user's location can be found in the sense of maximizing the uplink concurrent transmission probability $P_{CT}^{(u)}$.

Fig. 5 shows the impact of MS_2's locations on the uplink concurrent transmission probability $P_{CT}^{(u)}$. As shown in the figure, as the CR-based ad hoc user moves away from the BS, the concurrent transmission probability monotonically increases from 10 percent to 50 percent because the interference from the infrastructure-based link to the ad hoc connection decreases.

6.2 Downlink Concurrent Transmission Probability

Fig. 6 shows the downlink concurrent transmission probability $P_{CT}^{(d)}$ versus the distance r_3 of the primary user MS_3 to the BS when user MS_2 is located at $(50, -\pi/2)$. For the SIR requirement $z_i = z_a = 0$ dB, $P_{CT}^{(d)} = 25\%$ is a constant in the range of $r_3 \leq 100$ m. This is because the interference transmitted from the BS to the ad hoc users is independent of the locations of the primary user, MS_3. However, a more stringent SIR requirement $z_i = z_a = 3$ dB yields a lower and

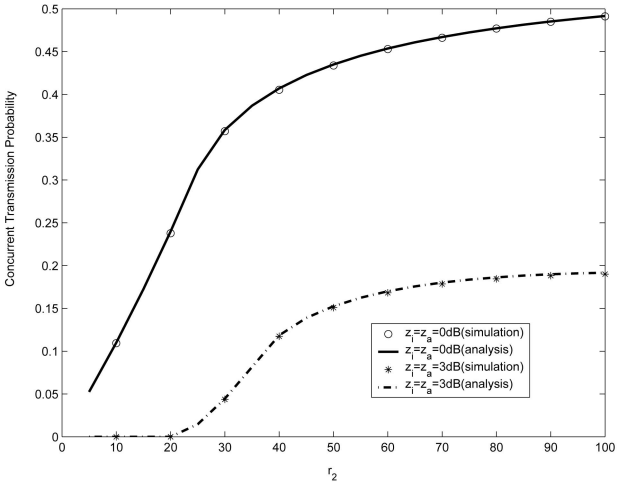

Fig. 5. The concurrent transmission probability $P_{CT}^{(u)}$ versus the CR-based ad hoc receiver's location as the infrastructure uplink user MS_3 is located at $(50, \pi/2)$, where r_2 is the distance between the BS and ad hoc link receiver MS_2.

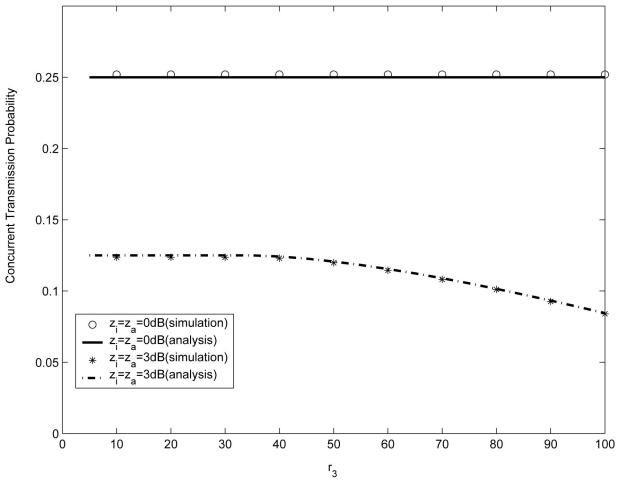

Fig. 6. Impact of primary user MS_3's location on the downlink concurrent transmission probability $P_{CT}^{(d)}$ as the ad hoc receiver MS_2 is located at $(50, -\pi/2)$.

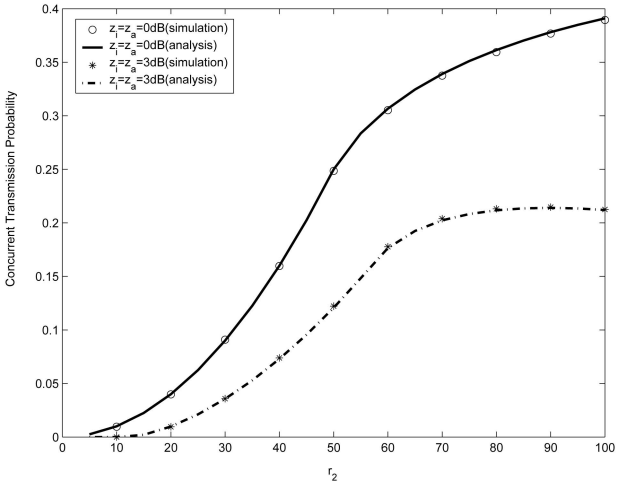

Fig. 7. Impact of CR-based ad hoc receiver MS_2's location on the concurrent transmission probability $P_{CT}^{(d)}$ as the infrastructure downlink user MS_3 is located at $(50, \pi/2)$.

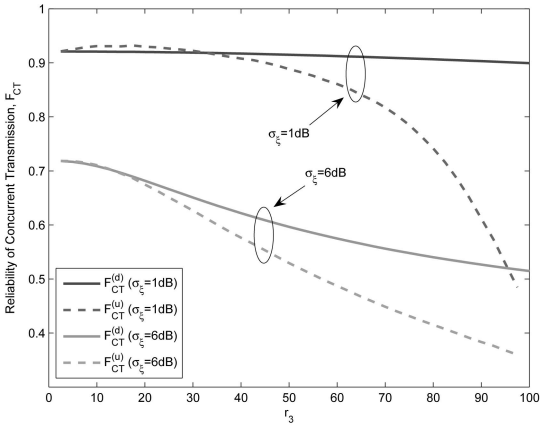

(a)

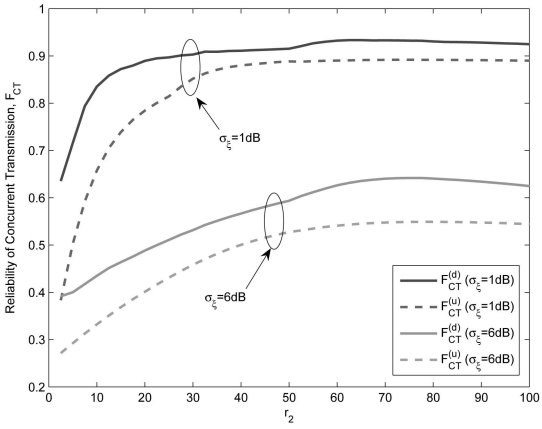

(b)

Fig. 8. Impacts of shadowing on the reliability of downlink $F_{CT}^{(d)}$ (solid line) and uplink $F_{CT}^{(u)}$ (dotted line) concurrent transmission against the locations of (a) the primary user MS_3 and (b) the ad hoc user MS_2 in the cases of $\sigma_\xi = 1$ and 6 dB, respectively.

decreasing downlink concurrent transmission probability when r_3 increases.

Fig. 7 shows the impact of CR user MS_2's locations on the downlink concurrent transmission probability. Similar to Fig. 5, $P_{CT}^{(d)}$ also monotonically increases when CR user MS_2 moves away from the BS. However, comparing Figs. 5 and 7, the uplink's concurrent transmission probability is higher than that of the downlink's. For $z_i = z_a = 0$ dB and $r_2 = 100$ m, $P_{CT}^{(u)} = 49$ percent and $P_{CT}^{(d)} = 39$ percent, respectively. This is because in the considered scenario the interference to the ad hoc user from the infrastructure-based uplink transmission is weaker than that from the downlink transmission.

6.3 Effects of Shadowing on the Concurrent Transmission

Figs. 8a and 8b illustrate the reliability of the concurrent transmissions with various shadowing standard deviations versus r_3 and r_2, respectively. In general, comparing $\sigma_\xi = 6$ dB and $\sigma_\xi = 1$ dB, one can find that the larger shadowing variance leads to a lower reliability for both uplink and downlink concurrent transmissions. For example, in Fig. 8a, when the primary user's distance to the BS r_3

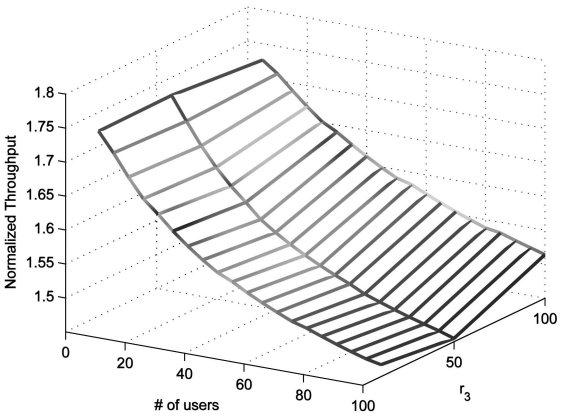

Fig. 9. Total throughput performance of the uplink concurrent transmission.

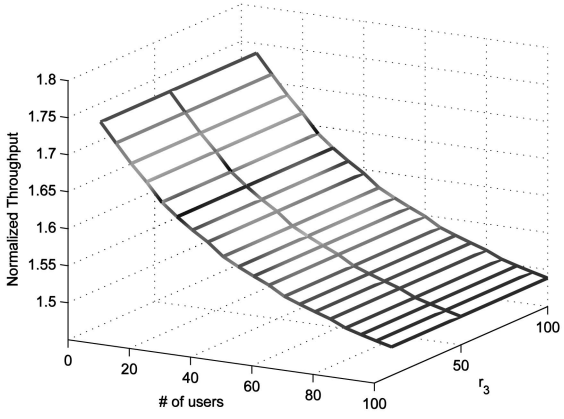

Fig. 10. Total throughput performance of the downlink concurrent transmission.

is in the range of $0 \sim 100$ m, $F_{CT}^{(d)}$ is larger than 0.9 for $\sigma_\xi = 1$ dB, whereas it decreases to $0.6 \sim 0.7$ for $\sigma_\xi = 6$ dB. However, when the primary user moves to the cell edge, the reliability of uplink and downlink concurrent transmissions decreases due to shadowing and weaker RSS. As shown in Fig. 8a, for $\sigma_\xi = 6$ dB, $F_{CT}^{(d)}$ and $F_{CT}^{(u)}$ decrease from 0.7 to 0.5 and 0.4, respectively. Since the uplink signal strength is weaker than the downlink signal, the reliability of uplink concurrent transmission is usually more sensitive to shadowing effects than downlink concurrent transmission, especially when the primary user is at the cell edge. In Fig. 8b, it is shown that, subject to the influence of shadowing, the reliability of uplink and downlink concurrent transmissions increases when the receiver MS_2 of the ad hoc link approaches the cell edge. For $\sigma_\xi = 1$ dB, $F_{CT}^{(u)}$ and $F_{CT}^{(d)}$ increase from 0.4 and 0.63 to 0.89 and 0.92 as r_2 increases to 100 m; for $\sigma_\xi = 6$ dB, $F_{CT}^{(u)}$ and $F_{CT}^{(d)}$ also increase from 0.29 and 0.4 to 0.54 and 0.62. Clearly, the interference from the primary user to the ad hoc user becomes weaker when ad hoc users moves away from the BS. As a result, the reliability of concurrent transmission increases and the shadowing effect on the reliability remains constant as $r_2 > 30$ m for $\sigma_\xi = 1$ dB and $r_2 > 60$ m for $\sigma_\xi = 6$ dB.

6.4 Total Throughput of Cognitive Ad Hoc Networks Overlaying Infrastructure-Based System with Concurrent Transmission

Fig. 9 demonstrates the total throughput of the CR-based ad hoc link and the infrastructure-based uplink transmissions for various numbers of ad hoc users and different locations of primary users. The total throughput is normalized to the infrastructure-based uplink capacity. As shown in the figure, in the worst case at $r_3 = 50$ m the total throughput with the concurrent transmission is still 145 percent higher than the pure infrastructure-based uplink, and the total throughput reaches a maximum of 173 percent at $r_3 = 10$ m.

Fig. 10 shows the total throughput performance of the concurrent transmission of infrastructure-based downlink and ad hoc link. In this case, the concurrent transmission probability is constant for various locations of primary users as shown in Fig. 6. Thus, the throughput is mainly affected by the number of ad hoc users. For $N_{CR} = 50$, the total throughput is 157 percent when $10 < r_3 < 100$ m. However, when $r_3 = 50$ m, the total throughput improves from 148 percent to 173 percent as N_{CR} is changed from 100 to 10.

7 Conclusions

In this paper, we identified a critical region R_{CT} in which the overlaying cognitive ad hoc users and the primary user can concurrently transmit data without causing interference to each other. If the location information of other nodes is available, such a concurrent transmission region can be easily identified. There are two major advantages of identifying the concurrent transmission opportunity. First, the overall throughput of the concurrently transmitted data obtained by combining both the overlaying cognitive ad hoc networks and the legacy infrastructure-based system is much higher than that of the pure infrastructure-based system. Our numerical results show that, in the uplink case, the concurrent transmission region subject to 1 and 6 dB shadowing standard deviation can be up to 45 percent out of the entire cell area with about 90 percent and 60 percent reliability, respectively. Second, if such a concurrent transmission opportunity can be identified first, it is clear that the need of the time- and energy-consuming wideband spectrum scanning process required by most existing CR systems can be reduced dramatically.

In summary, the results presented in this paper provide a design paradigm for CR systems from an alternative perspective—identifying spectrum opportunity cannot just rely on wideband spectrum sensing techniques. Location awareness also provides another important resource to help a CR system identify the opportunities of *concurrently using* the spectrum of the primary user in the spatial domain, instead of just *sharing* the spectrum in the time domain. It is hoped that our work has shed some light in this promising area of research. Nevertheless, there are still many unsolved open issues to realize the idea of exploiting the

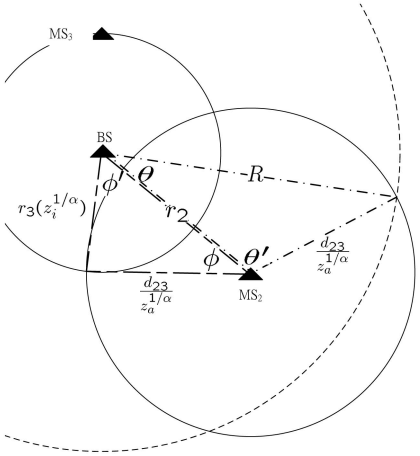

Fig. 11. Definition of parameters in the calculation of the area of region $R_{CT}^{(u)}$ in the infrastructure uplink case.

concurrent transmission opportunity by taking advantages of location awareness. Many interesting research topics, including the concurrent transmission MAC protocol design, the efficient mechanism of location information exchange, and the theoretical upper bound on the maximum concurrent transmission links overlaying the legacy infrastructure-based systems, are worthwhile to be investigated further.

APPENDIX A
DERIVATION OF (6)

The region $R_{CT}^{(u)}$ shown in (6) is composed of three sections with the areas of $\pi(d_{23}/z_a^{1/\alpha})^2$, A_1, and A_2. Fig. 11 shows all the parameters used in deriving the area of A_1 and A_2 in (7) and (8), respectively. In (7), section A_1 is composed of two fan-shaped areas with the measures of $(d_{23}/z_a^{1/\alpha})^2(\pi-\theta')$ and $R^2\theta$, and two identical triangles with the lengths of R, r_2, and $d_{23}/z_a^{1/\alpha}$, where

$$\theta = \cos^{-1}\frac{R^2 + r_2^2 - \frac{d_{23}}{z_a^{1/\alpha}}}{2Rr_2}, \tag{41}$$

$$\theta' = \cos^{-1}\frac{r_2^2 + \left(\frac{d_{23}}{z_a^{1/\alpha}}\right)^2 - R^2}{2r_2\left(\frac{d_{23}}{z_a^{1/\alpha}}\right)}, \tag{42}$$

$$\Delta = \sqrt{s(s-R)(s-r_2)\left(s-\frac{d_{23}}{z_a^{1/\alpha}}\right)}, \tag{43}$$

and

$$s = \frac{R + r_2 + \frac{d_{23}}{z_a^{1/\alpha}}}{2}. \tag{44}$$

Similarly, in (8), section A_2 is also made up of two fan-shaped areas with the measures of $(d_{23}/z_a^{1/\alpha})^2\phi$ and $(r_3 z_i^{1/\alpha})^2\phi'$, and the triangle with the lengths of r_2, $r_3 z_i^{1/\alpha}$, and $d_{23}/z_a^{1/\alpha}$, where

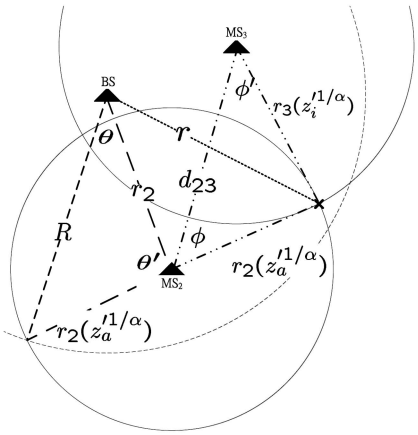

Fig. 12. Definition of parameters in the calculation of the area of region $R_{CT}^{(d)}$ in the infrastructure downlink case when $\max(r^+, r^-) \le R$.

$$\phi = \cos^{-1}\frac{r_2^2 + \left(\frac{d_{23}}{z_a^{1/\alpha}}\right)^2 - \left(r_3 z_i^{1/\alpha}\right)^2}{2r_2\left(\frac{d_{23}}{z_a^{1/\alpha}}\right)}, \tag{45}$$

$$\phi' = \cos^{-1}\frac{r_2^2 + \left(r_3 z_i^{1/\alpha}\right)^2 - \left(\frac{d_{23}}{z_a^{1/\alpha}}\right)^2}{2r_2\left(r_3 z_i^{1/\alpha}\right)}, \tag{46}$$

$$\Delta' = \sqrt{s'(s'-r_2)\left(s'-r_3 z_i^{1/\alpha}\right)\left(s'-\frac{d_{23}}{z_a^{1/\alpha}}\right)}, \tag{47}$$

and

$$s' = \frac{r_2 + r_3 z_i^{1/\alpha} + \frac{d_{23}}{z_a^{1/\alpha}}}{2}. \tag{48}$$

APPENDIX B
DERIVATION OF (12) AND (13)

The distances between the BS and the intersections by the two circles with the radii of $r_3 z_i'^{1/\alpha}$ and $r_2 z_a'^{1/\alpha}$ and centered at (r_3, θ_3) and (r_2, θ_2) are denoted by r^+ and r^-, respectively. Given the locations of intersections (x, y), they can be obtained by jointly solving the equations as follows:

$$\begin{cases} (x - r_2\cos\theta_2)^2 + (y - r_2\sin\theta_2)^2 = \left(r_2 z_a'^{1/\alpha}\right)^2, \\ (x - r_3\cos\theta_3)^2 + (y - r_3\sin\theta_3)^2 = \left(r_3 z_a'^{1/\alpha}\right)^2. \end{cases} \tag{49}$$

The distances between the BS and the intersections r^+ and r^-, respectively, shown in (12) and (13), can be obtained by solving the locations (x, y) from (49).

APPENDIX C
DERIVATION OF (15)

In the infrastructure downlink case, when $\max(r^+, r^-) \le R$, the region $R_{CT}^{(d)}$ is composed of three sections with the areas of $\pi(d_{23} z_a'^{1/\alpha})^2$, A_1, and A_2. Fig. 12 details the parameters used to calculate the areas of these sections in (16) and (17). In (16), the region A_1 is made up of two fan-shaped areas with the measures of $(r_2 z_a'^{1/\alpha})^2(\pi-\theta')$

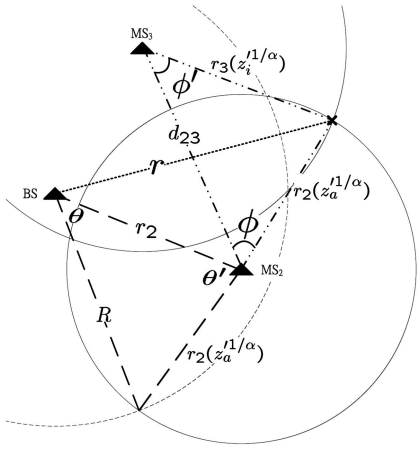

Fig. 13. Definition of parameters in the calculation of the areas of sections A_1 and A_2 in (18) in the infrastructure downlink case when $\max(r^+, r^-) > R$.

and $R^2\theta$, and two identical triangles with the lengths of R, r_2, and $r_2 z_a'^{1/\alpha}$, where

$$\theta = \cos^{-1}\frac{R^2 + r_2^2 - \left(r_2 z_a'^{1/\alpha}\right)}{2Rr_2}, \tag{50}$$

$$\theta' = \cos^{-1}\frac{r_2^2 + \left(r_2 z_a'^{1/\alpha}\right)^2 - R^2}{2r_2\left(r_2 z_a'^{1/\alpha}\right)}, \tag{51}$$

$$\Delta = \sqrt{s(s-R)(s-r_2)\left(s - r_2 z_a'^{1/\alpha}\right)}, \tag{52}$$

and

$$s = \frac{R + r_2 + r_2 z_a'^{1/\alpha}}{2}. \tag{53}$$

Similarly, section A_2 in (17) is also composed of two fan-shaped areas with the measures of $(r_2 z_a'^{1/\alpha})^2\phi$ and $(r_3 z_i'^{1/\alpha})^2\phi'$, and the triangle with the lengths of d_{23}, $r_2 z_a'^{1/\alpha}$, and $r_3 z_i'^{1/\alpha}$, where

$$\phi = \cos^{-1}\frac{d_{23}^2 + \left(r_2 z_a'^{1/\alpha}\right)^2 - \left(r_3 z_i'^{1/\alpha}\right)^2}{2d_{23}\left(r_2 z_a'^{1/\alpha}\right)}, \tag{54}$$

$$\phi' = \cos^{-1}\frac{d_{23}^2 + \left(r_3 z_i'^{1/\alpha}\right)^2 - \left(r_2 z_a'^{1/\alpha}\right)^2}{2d_{23}\left(r_3 z_i'^{1/\alpha}\right)}, \tag{55}$$

$$\Delta' = \sqrt{s'(s'-d_{23})\left(s' - r_3 z_i'^{1/\alpha}\right)\left(s' - r_2 z_a'^{1/\alpha}\right)}, \tag{56}$$

and

$$s' = \frac{d_{23} + r_2 z_a'^{1/\alpha} + r_3 z_i'^{1/\alpha}}{2}. \tag{57}$$

APPENDIX D
DERIVATION OF (18)

When $\max(r^+, r^-) > R$, the region $R_{CT}^{(d)}$ can be separated into four sections with the areas of $\pi(d_{23} z_a'^{1/\alpha})^2$, A_1, A_2, and A_3. Fig. 13 shows all the parameters in deriving (19), (20), and (21). In (19), section A_1 can be divided into two fan-shaped areas with the measures of $(r_2 z_a'^{1/\alpha})^2(\pi - \theta')$ and $R^2\theta$, and the triangle with the lengths of R, r_2, and $r_2 z_a'^{1/\alpha}$, where

$$\theta = \cos^{-1}\frac{R^2 + r_2^2 - \left(r_2 z_a'^{1/\alpha}\right)}{2Rr_2}, \tag{58}$$

$$\theta' = \cos^{-1}\frac{r_2^2 + \left(r_2 z_a'^{1/\alpha}\right)^2 - R^2}{2r_2\left(r_2 z_a'^{1/\alpha}\right)}, \tag{59}$$

$$\Delta = \sqrt{s(s-R)(s-r_2)\left(s - r_2 z_a'^{\frac{1}{\alpha}}\right)}, \tag{60}$$

and

$$s = \frac{R + r_2 + r_2 z_a'^{\frac{1}{\alpha}}}{2}. \tag{61}$$

In addition, section A_2 is made up of two fan-shaped areas with the measures of $(r_2 z_a'^{1/\alpha})^2\phi$ and $(r_3 z_i'^{1/\alpha})^2\phi'$, and the triangle with the lengths of d_{23}, $r_3 z_i'^{1/\alpha}$, and $r_2 z_a'^{1/\alpha}$, where

$$\phi = \cos^{-1}\frac{d_{23}^2 + \left(r_2 z_a'^{1/\alpha}\right)^2 - \left(r_3 z_i'^{1/\alpha}\right)^2}{2d_{23}\left(r_2 z_a'^{1/\alpha}\right)}, \tag{62}$$

$$\phi' = \cos^{-1}\frac{d_{23}^2 + \left(r_3 z_i'^{1/\alpha}\right)^2 - \left(r_2 z_a'^{1/\alpha}\right)^2}{2d_{23}\left(r_3 z_i'^{1/\alpha}\right)}, \tag{63}$$

$$\Delta' = \sqrt{s'(s'-d_{23})\left(s' - r_3 z_i'^{\frac{1}{\alpha}}\right)\left(s' - r_2 z_a'^{\frac{1}{\alpha}}\right)}, \tag{64}$$

and

$$s' = \frac{d_{23} + r_2 z_a'^{\frac{1}{\alpha}} + r_3 z_i'^{\frac{1}{\alpha}}}{2}. \tag{65}$$

At last, in (21), section A_3 is constructed by three arc-shaped areas with the measures of $(r_3 z_i'^{1/\alpha})^2\psi_2 - \left[(r_3 z_i'^{1/\alpha})^2 \sin\psi_2\right]/2$, $(r_2 z_a'^{1/\alpha})^2\psi_3 - \left[(r_2 z_a'^{1/\alpha})^2 \sin\psi_3\right]/2$, and $R^2\psi_1 - [R^2 \sin\psi_1]/2$, and the triangle with the lengths of a, b, and c, where

$$\begin{aligned}\psi_1 = {} & \cos^{-1}\frac{R^2 + r_2^2 - r_2^2 z_a'^{\frac{2}{\alpha}}}{2Rr_2} \\ & + \cos^{-1}\frac{R^2 + r_3^2 - r_3^2 z_i'^{\frac{2}{\alpha}}}{2Rr_3} \\ & - \cos^{-1}\frac{r_2^2 + r_3^2 - d_{23}^2}{2r_2 r_3},\end{aligned} \tag{66}$$

$$\begin{aligned}\psi_2 = {} & \cos^{-1}\frac{d_{23}^2 + r_3^2 z_i'^{\frac{2}{\alpha}} - r_2^2 z_a'^{\frac{2}{\alpha}}}{2d_{23}\left(r_3 z_i'^{\frac{1}{\alpha}}\right)} \\ & + \cos^{-1}\frac{d_{23}^2 + r_3^2 - r_2^2}{2d_{23}r_3} \\ & - \cos^{-1}\frac{r_3^2 + r_3^2 z_i'^{\frac{2}{\alpha}} - R^2}{2r_3\left(r_3 z_i'^{\frac{1}{\alpha}}\right)},\end{aligned} \tag{67}$$

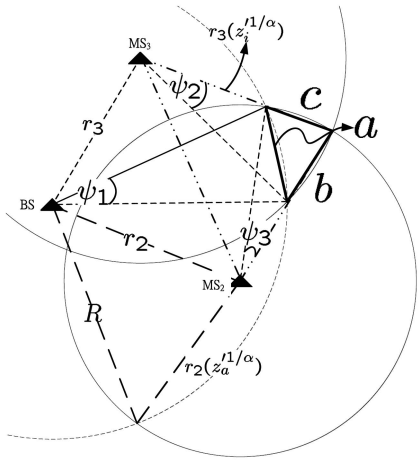

Fig. 14. Definitions of parameters in the calculation of the area of section A_3 in (18) in the infrastructure downlink case when $\max(r^+, r^-) > R$.

$$\psi_3 = \cos^{-1}\frac{d_{23}^2 + r_2^2 z_a^{\frac{2}{\alpha}} - r_3^2 z_i^{\frac{2}{\alpha}}}{2d_{23}\left(r_2 z_a^{\frac{1}{\alpha}}\right)} + \cos^{-1}\frac{d_{23}^2 + r_2^2 - r_3^2}{2d_{23}r_2} - \cos^{-1}\frac{r_2^2 + r_2^2 z_a^{\frac{2}{\alpha}} - R^2}{2r_2\left(r_2 z_a^{\frac{1}{\alpha}}\right)}, \quad (68)$$

$$\Delta'' = \sqrt{s''(s''-a)(s''-b)(s''-c)}, \quad (69)$$

$$s'' = \frac{a+b+c}{2}, \quad (70)$$

$$a = 2R\sin\frac{\psi_1}{2}, \quad (71)$$

$$b = 2\left(r_3 z i^{\frac{1}{\alpha}}\right)\sin\frac{\psi_2}{2}, \quad (72)$$

and

$$c = 2\left(r_2 z_a^{\frac{1}{\alpha}}\right)\sin\frac{\psi_3}{2}. \quad (73)$$

Fig. 14 shows all the parameters in deriving (21).

ACKNOWLEDGMENTS

This work was jointly supported by the National Science Council, Taiwan and the MOE ATU Program under Contracts NSC-96-2221-E-009-061, 96-2628-E-009-004-MY3, and 96W803, respectively.

REFERENCES

[1] E.M. Noam, "Taking the Next Step beyond Spectrum Auctions: Open Spectrum Access," *IEEE Comm. Magazine,* vol. 33, pp. 66-73, Dec. 1995.

[2] T.A. Weiss and F.K. Jondral, "Spectrum Pooling: An Innovative Strategy for the Enhancement of Spectrum Efficiency," *IEEE Comm. Magazine,* vol. 42, pp. s8-s14, Mar. 2004.

[3] F.C. Commission, *Notice of Proposed Rule Making and Order,* Report ET Docket 03-108, Dec. 2003.

[4] *The XG Vision,* http://www.darpa.mil/ato/programs/XG/, 2008.

[5] S. Haykin, "Cognitive Radio: Brain-Empowered Wireless Communications," *IEEE J. Selected Areas in Comm.,* vol. 23, no. 2, pp. 201-220, Feb. 2005.

[6] I.F. Akyildiz, W.Y. Lee, M.C. Vuran, and S. Mohanty, "NeXt Generation/Dynamic Spectrum Access/Cognitive Radio Wireless Networks: A Survey," *Computer Networks J.,* vol. 50, pp. 2127-2159, Sept. 2006.

[7] D. Cabric, S.M. Mishra, and R.W. Brodersen, "Implementation Issues in Spectrum Sensing for Cognitive Radios," *Proc. 38th Asilomar Conf. Signals, Systems, and Computers (ASILOMAR '04),* vol. 1, pp. 772-776, Nov. 2004.

[8] T. Weiss, J. Hillenbrand, A. Krohn, and F.K. Jondral, "Mutual Interference in OFDM-Based Spectrum Pooling Systems," *Proc. 59th IEEE Vehicular Technology Conf. (VTC '04),* vol. 4, pp. 1873-1877, May 2004.

[9] M. Oner and F. Jondral, "Extracting the Channel Allocation Information in a Spectrum Pooling System Exploiting Cyclostationarity," *Proc. 15th IEEE Int'l Symp. Personal, Indoors, and Mobile Radio Comm. (PIMRC '04),* vol. 1, pp. 551-555, Sept. 2004.

[10] F. Capar, I. Martoyo, T. Weiss, and F. Jondral, "Comparison of Bandwidth Utilization for Controlled and Uncontrolled Channel Assignment in a Spectrum Pooling System," *Proc. 55th IEEE Vehicular Technology Conf. (VTC '02),* vol. 3, pp. 1069-1073, May 2002.

[11] F. Capar, I. Martoyo, T. Weiss, and F. Jondral, "Analysis of Coexistence Strategies for Cellular and Wireless Local Area Networks," *Proc. 58th IEEE Vehicular Technology Conf. (VTC '03),* vol. 3, pp. 1812-1816, Oct. 2003.

[12] B. Aazhang, J. Lilleberg, and G. Middleton, "Spectrum Sharing in a Cellular System," *Proc. IEEE Int'l Symp. Spread Spectrum Techniques and Applications (ISSSTA '04),* pp. 355-359, Aug. 2004.

[13] T. Weiss, M. Spiering, and F.K. Jondral, "Quality of Service in Spectrum Pooling Systems," *Proc. 15th IEEE Int'l Symp. Personal, Indoors, and Mobile Radio Comm. (PIMRC '04),* vol. 1, pp. 345-349, Sept. 2004.

[14] Q. Zhao, L. Tong, and A. Swami, "Decentralized Cognitive MAC for Dynamic Spectrum Access," *Proc. First IEEE Int'l Symp. New Frontiers in Dynamic Spectrum Access Networks (DySPAN '05),* pp. 224-232, Nov. 2005.

[15] T.W. Rondeau, B. Le, C.J. Rieser, and C.W. Bostian, "Cognitive Radios with Genetic Algorithms: Intelligent Control of Software Defined Radios," *Proc. Software Defined Radio Forum Technical Conf. (SDR '04),* pp. C3-C8, 2004.

[16] Q. Zhao, L. Tong, and A. Swami, "A Cross-Layer Approach to Cognitive MAC for Spectrum Agility," *Proc. 39th IEEE Asilomar Conf. Signals, Systems, and Computers (ASILOMAR '05),* pp. 200-204, Nov. 2005.

[17] S. Krishnamurthy, M. Thoppian, S. Venkatesan, and R. Prakash, "Control Channel Based MAC-Layer Configuration, Routing and Situation Awareness for Radio Networks," *Proc. IEEE Military Comm. Conf. (MILCOM '05),* pp. 1-6, Oct. 2005.

[18] C. Doerr, M. Neufeld, J. Fifield, T. Weingart, D.C. Sicker, and D. Grunwald, "MultiMAC—An Adaptive MAC Framework for Dynamic Radio Networking," *Proc. First IEEE Int'l Symp. New Frontiers in Dynamic Spectrum Access Networks (DySPAN '05),* pp. 548-555, Nov. 2005.

[19] S. Sankaranarayanan, P. Papadimitratos, A. Mishra, and S. Hershey, "A Bandwidth Sharing Approach to Improve Licensed Spectrum Utilization," *Proc. First IEEE Int'l Symp. New Frontiers in Dynamic Spectrum Access Networks (DySPAN '05),* pp. 279-288, Nov. 2005.

[20] Y. Xing and R. Chandramouli, "Dynamic Spectrum Access in Open Spectrum Wireless Networks," *IEEE J. Selected Areas in Comm.,* vol. 24, pp. 626-637, Mar. 2006.

[21] H. Wu, C. Qiao, S. De, and O. Tonguz, "Integrated Cellular and Ad Hoc Relaying Systems: iCAR," *IEEE J. Selected Areas in Comm.,* vol. 19, no. 10, pp. 2105-2115, Oct. 2001.

[22] E. Yanmaz, O.K. Tonguz, S. Mishra, H. Wu, and C. Qiao, "Efficient Dynamic Load Balancing Algorithms Using iCAR Systems: A Generalized Framework," *Proc. 56th IEEE Vehicular Technology Conf. (VTC '02),* vol. 1, pp. 586-590, Sept. 2002.

[23] E.H.-K. Wu, Y.-Z. Huang, and J.-H. Chiang, "Dynamic Adaptive Routing for Heterogeneous Wireless Network," *Proc. IEEE Global Telecomm. Conf. (GLOBECOM '01),* vol. 6, pp. 3608-3612, Nov. 2001.

[24] Y.D. Lin and Y.C. Hsu, "Multihop Cellular: A New Architecture for Wireless Communications," *Proc. IEEE INFOCOM,* vol. 3, pp. 26-30, Mar. 2000.
[25] J. Chen, S.-H.G. Chan, J. He, and S.C. Liew, "Mixed-Mode WLAN: The Integration of Ad-Hoc Mode with Wireless LAN Infrastructure," *Proc. IEEE Global Telecomm. Conf. (GLOBECOM '03),* vol. 1, pp. 231-235, Dec. 2003.
[26] D. Niculescu and B. Nath, "Ad Hoc Positioning System (APS)," *Proc. IEEE INFOCOM,* vol. 3, pp. 1734-1743, Mar. 2001.
[27] J. Hightower and G. Borriello, "Location Systems for Ubiquitous Computing," *Computer,* vol. 34, no. 8, pp. 57-66, Aug. 2001.
[28] D. Niculescu and B. Nath, "Ad Hoc Positioning System (APS) Using AOA," *Proc. IEEE INFOCOM,* vol. 3, pp. 1734-1743, Mar. 2003.
[29] S.J. Ingram, D. Harmer, and M. Quinlan, "Ultrawideband Indoor Positioning Systems and Their Use in Emergencies," *Proc. Position Location and Navigation Symp. (PLANS '04),* pp. 706-715, Apr. 2004.
[30] D. Madigan, E. Einahrawy, R.P. Martin, W.-H. Ju, P. Krishnan, and A.S. Krishnakumar, "Bayesian Indoor Positioning Systems," *Proc. IEEE INFOCOM,* vol. 2, pp. 1217-1227, Mar. 2005.
[31] G. Sun, J. Chen, W. Guo, and K.-J.R. Liu, "Signal Processing Techniques in Network-Aided Positioning: A Survey of State-of-the-Art Positioning Designs," *IEEE Signal Processing Magazine,* vol. 22, no. 4, pp. 12-23, July 2005.
[32] Y.-C. Tseng, S.-L. Wu, W.-H. Liao, and C.-M. Chao, "Location Awareness in Ad Hoc Wireless Mobile Networks," *Computer,* vol. 34, no. 6, pp. 46-52, June 2001.
[33] M. Mauve, A. Widmer, and H. Hartenstein, "A Survey on Position-Based Routing in Mobile Ad Hoc Networks," *IEEE Network,* vol. 15, no. 6, pp. 30-39, Nov./Dec. 2001.
[34] X. Hong, K. Xu, and M. Gerla, "Scalable Routing Protocols for Mobile Ad Hoc Networks," *IEEE Network,* vol. 16, no. 4, pp. 11-21, July/Aug. 2002.
[35] T. Park and K.G. Shin, "Optimal Tradeoffs for Location-Based Routing in Large-Scale Ad Hoc Networks," *IEEE/ACM Trans. Networking,* vol. 13, no. 2, pp. 398-410, Apr. 2005.
[36] H. Celebi and H. Arslan, "Adaptive Positioning Systems for Cognitive Radios," *Proc. IEEE Int'l Symp. New Frontiers in Dynamic Spectrum Access Networks (DySPAN '07),* pp. 78-84, Apr. 2007.
[37] T.S. Rappaport, *Wireless Communications: Principle and Practice,* second ed. Prentice Hall, 2002.
[38] G.L. Stüber, *Principle of Mobile Communication,* second ed. Kluwer Academic, 2001.
[39] G. Bianchi, "Performance Analysis of IEEE 802.11 Distributed Coordination Function," *IEEE J. Selected Areas in Comm.,* vol. 18, no. 3, pp. 535-547, Mar. 2000.
[40] L.C. Wang, S.Y. Huang, and A. Chen, "A Cross-Layer Throughput Performance Investigation for CSMA/CA-Based Wireless Local Area Network with Directional Antennas and Capture Effect," *Proc. IEEE Wireless Comm. and Networking Conf. (WCNC '04),* vol. 3, pp. 1879-1884, Mar. 2004.

Li-Chun Wang received the BS degree in electrical engineering from the National Chiao-Tung University, Hsinchu, Taiwan, in 1986, the MS degree in electrical engineering from the National Taiwan University, Taipei, in 1988, and the MSc and PhD degrees in electrical engineering from Georgia Institute of Technology, Atlanta, in 1995 and 1996, respectively. From 1990 to 1992, he was with Chunghwa Telecom. In 1995, he was with Northern Telecom, Richardson, Texas. From 1996 to 2000, he was with AT&T Laboratories, where he was a senior technical staff member in the Wireless Communications Research Department. Since August 2000, he has been an associate professor in the Department of Communication Engineering, National Chiao-Tung University, where he has been a full professor since August 2005. He was a corecipient of the Jack Neubauer Best Paper Award from the IEEE Vehicular Technology Society in 1997. His current research interests are in the areas of cellular architectures, radio network resource management, and cross-layer optimization for cooperative and cognitive wireless networks. He is the holder of three US patents with three more pending. He is a senior member of the IEEE.

Anderson Chen received the BS, MS, and PhD degrees in communication engineering from the National Chiao-Tung University, Hsinchu, Taiwan, in 1998, 1999, and 2007, respectively. He is currently working on his national service. His research interests include wireless networks, cross-layer design, and cognitive wireless system. He is the holder of a US patent with three more pending. He is a student member of the IEEE.